

The pictures in this pdf
file have been reduced
to 72 dpi

8 WAVES

Erosion and stability



Dike with basalt columns and concrete blocks (Zeeland),
courtesy Rijkswaterstaat

8.1 Erosion

Before considering the necessity of protecting a bank, a shore or a bottom against waves, one should have an idea of the possible erosion. In this book, erosion due to waves is limited to local erosion. For banks and shores this will be treated on the basis of beach and dune erosion research; for bottom erosion, breakwater investigations will be used. Erosion due to long-shore or cross-shore sediment transport is part of coastal morphology and will not be treated.

8.1.1 Erosion of slopes

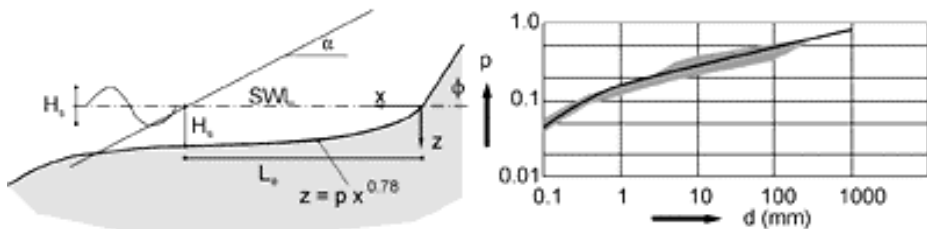


Figure 8-1 Erosion of slope by waves

Waves acting on an unprotected slope cause a step profile. This is the natural equilibrium profile for all slopes composed of loose material (see e.g. Vellinga, 1986). Theoretically, monochromatic waves lead to a parabolic beach with $z \propto x^{2/3}$. For practical situations, Vellinga proposes:

$$z = 0.39 w^{0.44} x^{0.78} = p x^{0.78} \quad (8.1)$$

in which w is the fall velocity of the particles; for the definition of z and x , see Figure 8-1. p is expressed in $\text{m}^{0.22}$!

This is an equilibrium profile; development in time is not considered. The erosion depth below SWL is about H_s . From equation (8.1) the intrusion length of the waves in the profile is then found by:

$$L_e = p^{-1.28} H_s^{1.28} \quad (8.2)$$

Above the still water level the slope is assumed to be equal to the angle of repose. Figure 8-1 gives a relation for the value of p in the profile formula. The given relations can serve only as a first indication and should be applied for wave attack well beyond the limit of stability, see section 8.3.2.

Example 8-1

A sand slope, with grain size 0.5 mm, is temporarily unprotected. What is the erosion length if this slope is attacked by waves with $H_s = 1.6$ m?

From Figure 8-1 we find for grains of 0.5 mm, $p \approx 0.1$. From equation 8.2 we then find: $L_e = 0.1^{-1.28} * 1.6^{1.28} \approx 35$ m.

8.1.2 Bottom erosion

Bottom scour due to waves can be important in front of walls where a standing wave pattern is possible. From chapter 7 we know that the highest velocities occur in the nodes of such a wave and indeed, for fine sediments, the maximum scour is found there. For coarse sediments, however, the maximum scour is found between the node and antinode, probably due to a different eddy and ripple pattern. The standing wave pattern for irregular waves is less distinct than for regular waves. This is also found in the scouring pattern, which decreases strongly with the distance from the wall, see Figure 8-2a and b.

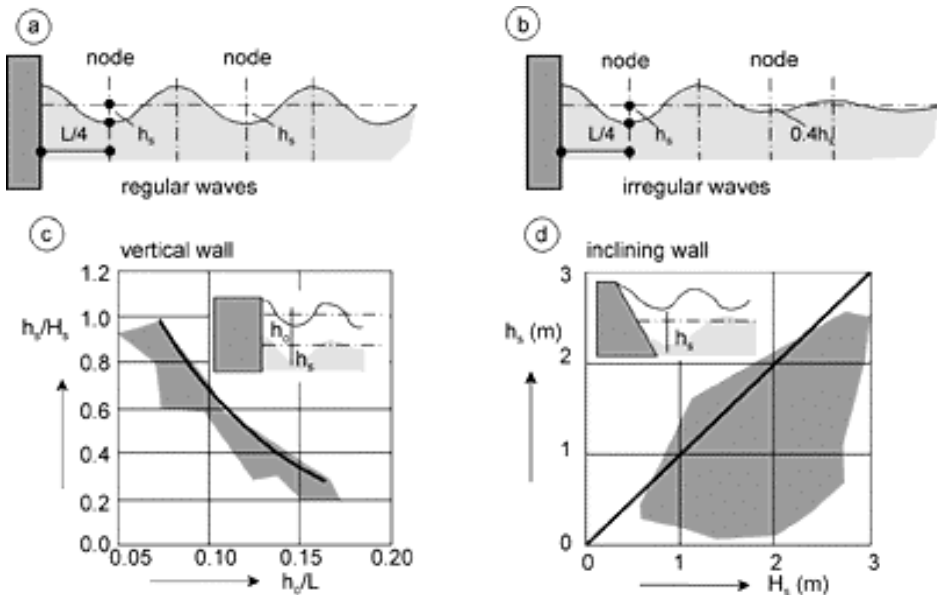


Figure 8-2 Bottom erosion in front of wall due to waves

The depth of the scour hole can be estimated roughly with Figure 8-2c (from Xie Shi-Leng, 1981). For shallow water (small h_0/L), $h_s \approx H_s$ can serve as a first guess. For deeper water, the scour is considerably less.

When the wall is not vertical but inclining, the maximum scour will occur at the foot of the wall, due to the backflow from the sloping wall, see Figure 8-2d. The erosion is roughly proportional to the reflection coefficient, so a vertical wall gives maximum values. As a first guess for all cases, $h_s \approx H_s$ can be used as an upper limit.

8.2 Stability general

Several stable protections against waves are possible. In this book they will be divided into three main categories, with the following keywords:

- 1 Loose grains, rip-rap, rock, open, permeable.
- 2 Coherent, semi-permeable, placed block revetment.
- 3 Impervious, asphalt, concrete.

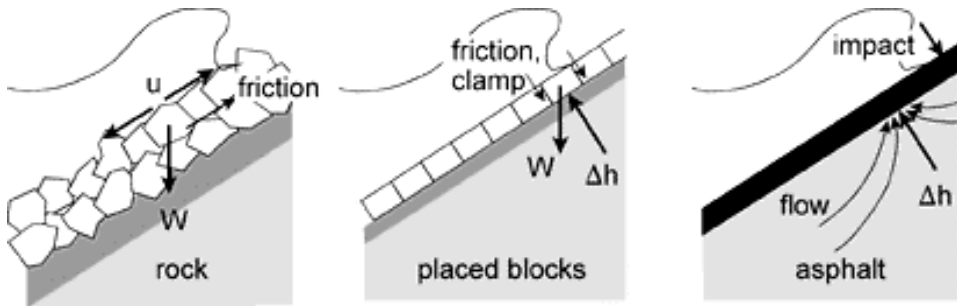


Figure 8-3 Three main types of protection against waves

The loads on these three archetypes of protection are the same, but completely different mechanisms determine the dimensions of the protection layers. The differences lie in the transfer functions from the external to the internal load and from the internal load to the response of the structure (strength). This can be illustrated by considering the so-called leakage length, Λ .



Figure 8-4 Definition leakage length

Consider the flow in Figure 8-4a. In the filter layer, the flow is assumed to be parallel to the interface, while in the top layer it is perpendicular. When there is no filter layer (Figure 8-4b), some assumption has to be made for the thickness where parallel flow can be expected. These assumptions may not be completely true for all revetment types in Figure 8-3, but the concept is used for illustration purposes only.

Starting with these flow directions, the flow resistance of each layer can be determined. The leakage length, Λ , is now defined as the length of protection in which the flow resistance through top layer and filter layer are the same, see Figure 8-4a. This definition can be expressed by (see also De Groot et al., 1988):

$$\frac{d_T}{k_T \Lambda} = \frac{\Lambda}{k_F d_F} \rightarrow \Lambda = \sqrt{\frac{k_F d_F d_T}{k_T}} \quad (8.3)$$

in which k_F and k_T are the permeability of filter and top layer, respectively, and d_F and d_T the thickness. So, a large leakage length means a relatively impermeable top layer compared with the filter layer.

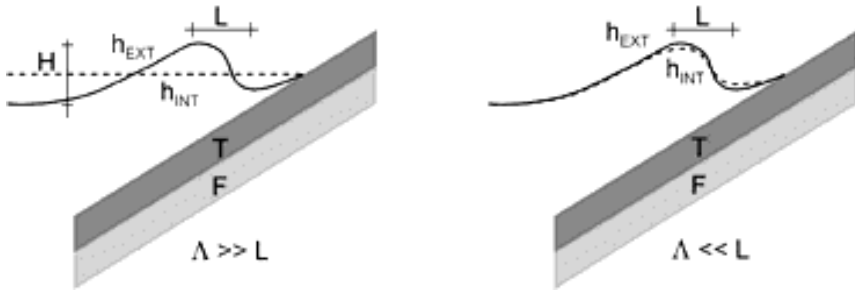


Figure 8-5 Influence leakage length

Λ is a measure for the exchange between external and internal loads, see Figure 8-5. L is some characteristic length of the external load (not necessarily the wave length, but e.g. the length of the wave front). When $\Lambda \gg L$, there is little exchange between the outside and the inside and the piezometric level inside the filter cannot follow the level outside, leading to a large head-difference. When $\Lambda \ll L$, the exchange is easy and there is hardly any head-difference: the pressure gradients in the load are only determined by L .

Table 8-1 Typical values for Λ and L for different protection types

Parameter	"Rock"	"Blocks"	"Asphalt"
d_T (m)	0.5	0.25	0.25
d_F (m)	0.25	0.2	2
k_T (m/s)	0.5	0.001	"0"
K_F (m/s)	0.1	0.05	0.0001
Λ (m)	0.15	1.5	" ∞ "
L (m)	1-2	1-2	1-2

Table 8-1 gives some typical values for the three protection types of Figure 8-3. For a protection of loose rock $\Lambda \ll L$, for a placed block revetment $\Lambda \approx L$ and for an asphalt protection $\Lambda \gg L$. This may explain why these protections behave completely differently, while the strength is also different.

In the case of loose rock, $\Lambda \ll L$ and there is no head difference across the top layer. L determines the pressure gradients, leading to uprush and downflow velocities,

which in turn cause (drag)forces on the individual stones. **Note:** Obviously, the assumption of flow perpendicular to the top layer (Figure 8-4) is no longer valid. The strength of this revetment is a result of friction between the stones, hence of their weight, see Figure 8-3a. Porous flow has some influence on the stability, but this is of minor importance compared with the external flow forces. Thus, the stability of a slope with a rock top-layer is governed by the flow caused by the waves around the stones, analogous to the stability in flow as described in chapter 3. Section 8.3 deals with stability of loose grains. A filter is usually necessary for stability, since the top layer is very open and the underlying grains can be washed away without the filter. For an impervious protection, $\Lambda \gg L$ and the head-difference across the top layer is approximately $H/2$, see Figure 8-5. However, the transfer function from the wave load to the response of the asphalt layer is such that this load is usually negligible. The head difference causes a force which will try to lift the protection layer. The load is local while the layer is coherent and heavy and, as a consequence, difficult to move. Moreover, the cavity between protection and subsoil has to be filled with water within part of a wave period, for which the porous flow is usually not fast enough. Wave impact can cause damage, if it occurs very frequently, see section 8.4.2. The stability of the layer is governed by the pressure differences due to variations in the waterlevel as described in chapter 5. A filter for sandtightness is unnecessary. A filter for drainage can be applied when the phreatic level inside the slope, due to tides or surges, will cause high pressures under the revetment. In the case of placed blocks, $\Lambda \approx L$. In the cases where $\Lambda \gg L$ or $\Lambda \ll L$, it is possible to focus on a dominant mechanism, but when $\Lambda \approx L$, the situation is more complex. The surface is usually too smooth for the water to exert drag forces. The load comes from inside, caused by the pressure difference under and above the blocks. The strength is the result of the cooperation between the blocks, either by friction or by clamping. Now the porous flow is paramount for the stability and the filter plays a crucial and complex role, see section 8.4.1.

8.3 Stability of loose grains

As a logical continuation of chapter 3 (Stability in flow), we will start to examine the stability of loose material under waves and pretend that the loading situation and stability under waves are not different from those in flow. After all, the water in a non breaking wave, is just flowing to and fro, albeit with a higher shear stress. In breaking waves, we can not expect this approach to be succesful in a quantitative way, but it is always instructive to try and compare the results.

8.3.1 Stability in non-breaking waves

Chapter 7 gave Jonsson's expression for the shear stress under a wave and with this shear stress we could use the stability relation for flow, e.g. the one by Shields,

which relates the dimensionless shear stress to the grain diameter. The results of this approach deviate from the original Shield's results, probably due to different boundary development in an oscillating flow. Figure 8-6a shows stability measurements in oscillating flow presented by various authors, summarized by Sleath, 1978.

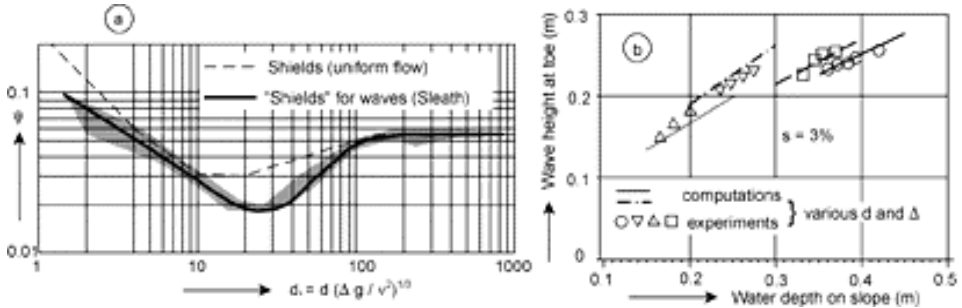


Figure 8-6 Modified Shields-diagram for waves and stability in non-breaking waves

Sleath uses the same dimensionless shear stress as Shields does (ψ), and the same dimensionless grain diameter as Van Rijn for flow, see chapter 3. So, the results can be compared directly, see Figure 8-6a. For large d_* (turbulent boundary layer), Sleath found a value for ψ to be 0.055, which is almost the same value as Shields. In stationary flow, this value implies a relatively large amount of stones in motion. How logical is it that the same value is found in oscillating flow? Two factors can play a role. The criterion for the threshold of movement in oscillating flow is not quite clear, but a potentially unstable stone in oscillating flow can not move a long distance, hence the subjective threshold will probably be assumed rather high compared with the threshold in steady flow. Another aspect may be the phenomenon we have seen in an accelerating steady flow, which is that ψ increases as τ increases. The graph by Sleath is based on several investigations. One of them is by Rance/Warren, 1968. Their results can be summarized by the equation (see Schiereck et al., 1996):

$$\frac{a_b}{T^2 \Delta g} = 0.025 \left(\frac{a_b}{d_{50}} \right) \rightarrow d_{n50} = 2.15 \frac{\hat{u}_b^{2.5}}{\sqrt{T} (\Delta g)^{1.5}} \quad (8.4)$$

in which a_b is the orbital stroke at the bottom and \hat{u}_b the maximum orbital velocity, where d_{n50} is assumed to equal $0.84d_{50}$. Equation (8.4) has the advantage that no iteration is necessary between the bottom roughness and the shear stress as is the case in the Jonsson-Sleath approach.

Figure 8-6b shows a comparison between stability calculations with orbital velocities from linear wave theory, Jonsson's friction factor and $\psi = 0.055$ for stones on a slope 1:25 and laboratory tests with regular non-breaking waves, see Schiereck et al, 1994.

The computed wave heights at the toe of the slope, for which the material starts to move, correspond quite good with the measured values. Equation (8.4) gives similar results.

8.3.2 Stability in breaking waves

Most research on the stability of stones on a slope has been carried out in the field of breakwaters, which is very much related to slope protections and revetments, but it is not the same. An important difference in the stability is the porosity of the entire structure. Breakwaters usually have a porous core, while in dike revetments the core is made of clay or sand. This has a significant influence on the stability of the protecting armour layer as we will see later on in this section. We will start, however, with basic principles and shortcomings and extensions will be discussed later on.

Encouraged by the successful results of the modified Shields-curve for waves, the next step is using a slope correction factor and taking the breaking of the waves into account. We will use the same slope factor as for flow in the slope direction (see section 3.3. For the 1:25 slope in the previous section, this factor ≈ 1). For the velocity in a breaking wave, no reliable expression is available. As a first guess, we will assume that the velocity in a breaking or broken wave on a slope is proportional to the celerity in shallow water with the wave height as a representative measure for the waterdepth: $u \propto \sqrt{gH}$. Following the same reasoning as for stability in flow, see chapter 3, we find:

$$\begin{array}{lll} \rho_w g H d^2 & \propto & (\rho_s - \rho_w) g d^3 \quad (\tan \phi \cos \alpha \pm \sin \alpha) \\ \text{"drag" force} & & \text{resisting force} \quad \text{slope correction} \end{array} \quad (8.5)$$

Note: + and - in the slope correction are for uprush and backwash, respectively. By raising all terms to the third power and working with the mass of the stone ($M \propto \rho_s d^3$) we find, as was already proposed by Iribarren, 1938:

$$M \propto \frac{\rho_s H^3}{\Delta^3 (\tan \phi \cos \alpha \pm \sin \alpha)^3} \quad (8.6)$$

Many tests were performed (mostly by Hudson, 1953) to find the constants of proportionality in equation (8.6). For practical reasons, Hudson finally proposed another formula:

$$M = \frac{\rho_s H_{sc}^3}{K_D \Delta^3 \cot \alpha} \quad (\text{or: } \frac{H_{sc}}{\Delta d} = \sqrt[3]{K_D \cot \alpha}) \quad (8.7)$$

Note: The use of $H_{sc}/\Delta d$ as a stability parameter is convenient and it resembles the stability parameter in flow situations, $u_c^2/\Delta d$. The subscript c in the stability parameter (to discern stability from mobility) is not always used consequently.

The slope correction in Iribarren's formula is now reduced to $\cot \alpha$. This means that the validity of Hudson's formula is limited, because $\cot \alpha$ is insufficient to describe friction and equilibrium on a slope: when $\alpha = 0$, $M = 0$ and when $\alpha > \phi$, M still has a finite value, which is nonsense. The range of α for which Hudson is valid is about $1.5 < \cot \alpha < 4$. The Hudson-formula was tested for waves that did not break at the toe of the slope and did not overtop it. For other cases, extra corrections for K_D are sometimes applied. Hudson's formula is simple and is used worldwide. K_D is again a 'dustbin-factor' in which the accepted degree of damage is implicitly included. K_D has different values for different kinds of elements (3-4 for natural rock to 8-10 for artificial elements like tetrapods and tribars). The Shore Protection Manual (SPM, 1984) gives values for K_D for various circumstances. The simplicity of the Hudson-formula has its price. Some limitations of the presented formulae have already been mentioned. The most important limitations are:

Wave period

In the Iribarren-formula this parameter is absent. There are two ways in which the period influences the stability. On the one hand, the period is related to the wavelength, hence to the wave steepness and hence to the breaking pattern on the slope, which definitely plays a role. On the other hand, inertia forces on a grain may play a role, which depend on du / dt , hence on the wave period.

Permeability

The permeability of the structure must play an important role. The assumptions on which Iribarren's formula is based, only include a kind of drag force on the slope. The forces under and behind a grain are certainly partly responsible for the equilibrium. It is easy to imagine that a homogeneous mass of stones reacts differently from a cover layer of stones on an impermeable core. In the first case, a lot of wave energy is dissipated in the core, while in the latter the pressure build-up under the cover layer can be considerable.

Number of waves

All model tests in the fifties and sixties were carried out with regular waves. In those tests it appeared that the equilibrium damage-profile was reached in, say, one half hour. The wave height in the tests was then usually declared to be equivalent to H_s . It appeared from tests with wave spectra that the number of waves has some influence, which is logical, as more waves mean a greater chance of a large one occurring.

Damage level

As for stones in flow, the threshold of motion for stones in waves is not always clear. The K_D -values in the Hudson-formula are supposed to be valid for 5% damage, but the definition of damage is not very clear.

All these objections have led to new research activities, which have increased following some failures of breakwaters. In a period of about ten years the recommended coefficients for the Hudson formula in the Shore Protection Manual for breakwater design have increased by about 200%. In The Netherlands, extensive model tests were carried out to overcome the limitations of the Hudson-formula. The results of curve-fitting the outcome of these large and small scale tests with irregular waves, finally led to the following equations, see Van der Meer, 1988:

$$\frac{H_{sc}}{\Delta d_{n50}} = 6.2 P^{0.18} \left(\frac{S}{\sqrt{N}} \right)^{0.2} \xi^{-0.5} \quad (\text{plunging breakers})$$

$$\frac{H_{sc}}{\Delta d_{n50}} = 1.0 P^{-0.13} \left(\frac{S}{\sqrt{N}} \right)^{0.2} \xi^P \sqrt{\cot \alpha} \quad (\text{surging breakers})$$
(8.8)

in which: P is a measure for the permeability of the structure, S a measure for the damage and N the number of waves. The transition between the two expressions is found by equating them, giving:

$$\xi_{\text{transition}} = \left[6.2 P^{0.31} \sqrt{\tan \alpha} \right] \left(\frac{1}{P+0.5} \right)$$
(8.9)

When $\xi > \xi_{\text{transition}}$ the equation for surging breakers has to be used, for $\xi < \xi_{\text{transition}}$, the equation for plunging breakers. In practice, for $\cot \alpha \geq 4$ surging waves do not exist and only the expression for plunging waves is recommended for use.

Compared with Hudson's equation, these equations are a step forward, because more parameters are included. The physical base of the Van der Meer equations is, however, still weak and in stone stability under waves there is still much to be understood. As a stability parameter Van der Meer used $H_s/\Delta d_{n50}$ (see also equation (8.7)), the wave-period appears in the surf-similarity parameter, ξ_m (m means related to the average wave period), while there is a discontinuity in the stability relations between surging and plunging breakers. In the following the influence of the parameters in equations (8.8) will be demonstrated with some computations and a comparison with the Hudson-formula. A standard case will be used:

$H_s = 2 \text{ m}$	$T_m = 6 \text{ s}$	$\Delta = 1.65$
$\cot \alpha = 3$	$N = 3000$	$S = 2$
$P = 0.5$	$d_{n50} = 0.6 \text{ m (300 - 1000 kg)}$	$K_D = 3.5$

Wave period

The influence of the wave period is incorporated in the breaker parameter, ξ . Figure 8-7a shows the relation between the stability parameter, $H_s / \Delta d_{n50}$, and ξ (with all other parameters as in the standard case). Near $\xi = 3$, $H_s / \Delta d$ has its minimum. This is in the transition zone between surging and plunging breakers, which appears to give the most severe attack on the slope, see also chapter 7. Note that typical values of $H_s / \Delta d$ lie around 2 for both formulae. Below $\xi = 1$, the Van der Meer curve is dashed, since the empirical relation was not tested for those values, see also Figure 8-13. In Figure 8-7b the period is the independent parameter. Note that periods smaller than 4 s have not been drawn, since a maximum wave steepness ($s = H_s / L_0$) = 0.06 has been assumed, which, with a wave height of 2 m, leads to a minimum wave period of $\approx 3\sqrt{H_s}$. In the Hudson-formula, T does not play a role.

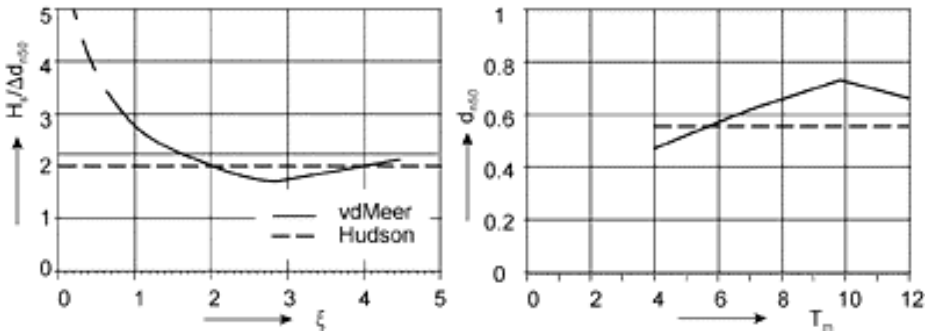


Figure 8-7 Stability parameter as a function of ξ and diameter as function of T

Permeability

A permeability parameter P has been introduced and the value for different structures has been established by curve-fitting the results. Figure 8-8a gives the values for various situations. A homogeneous structure (no core) gives $P \approx 0.6$, a rock armour-layer with a permeable core ($d_A / d_F \approx 3$): $P \approx 0.5$, an armour layer with filter ($d_A / d_F \approx 2$) on a permeable core ($d_F / d_C \approx 4$): $P \approx 0.4$ and an "impermeable" core: $P \approx 0.1$. Impermeable is again a relative notion, wave penetration in clay or even sand is almost negligible, so, in these stability relations the slope is considered impermeable. Attempts have been made to derive P from porous flow calculations, see Van Gent, 1993.

Figure 8-8b shows the influence of P on the necessary diameter. For permeable slopes, the results from Hudson or Van der Meer are almost identical, but for impermeable slopes, like dikes or revetments, the difference is considerable (0.75 m versus 0.55 m, which is a 2.5 times heavier stone).

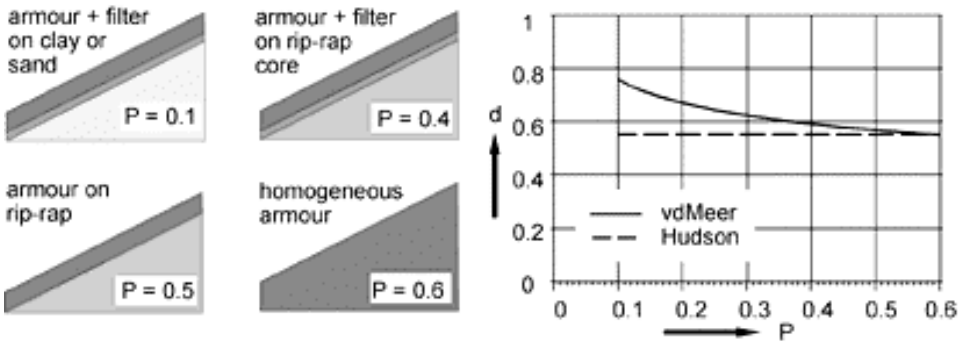


Figure 8-8 Stone diameter as a function of slope permeability

Number of waves

N is the number of waves. Figure 8-9 gives the increase of the damage with the number of waves during a test. With $N = 7500$, the damage can be considered to have reached an equilibrium. When only storms of short duration occur and intensive maintenance will be done, a smaller N can be chosen, leading to a smaller d , which is possibly cheaper. 3000 waves with an average period of 6 s, represent a storm of 5 hours.

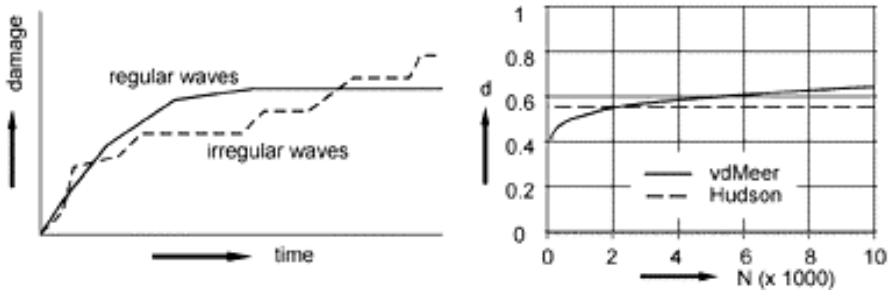


Figure 8-9 Damage versus time and stone diameter versus number of waves

Damage level

The damage level has been defined in a more manageable way, see Figure 8-10a: $S = A_e / d^2$. This is an erosion area divided by the square of the stone diameter. In a strip with a width d perpendicular to the page, S is more or less equal to the number of removed stones. The advantage of S is the use of an area which can be objectively measured by soundings. For the threshold of damage, $S = 2-3$, can be used. When the armor layer is locally completely removed and the filter layer becomes exposed, the damage can be defined as failure of the structure. Depending on the slope, the matching S is about 10.

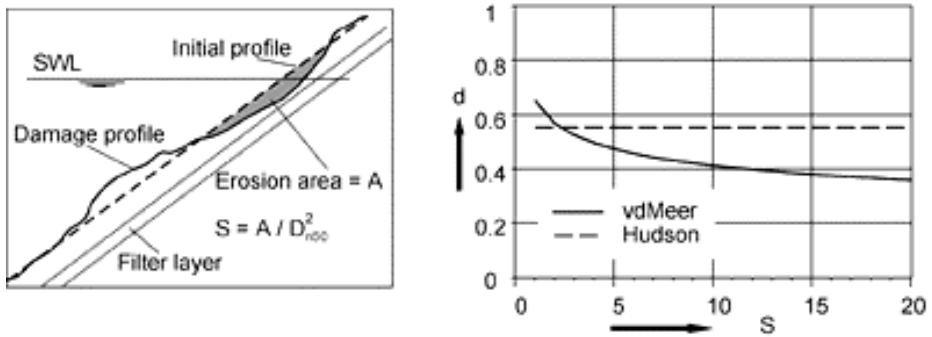


Figure 8-10 Stone diameter as a function of the damage level

Wave height and slope angle α

Figure 8-11, finally, shows the influence of the wave height and of the slope angle. For these two parameters, Hudson and Van der Meer show the same tendency.

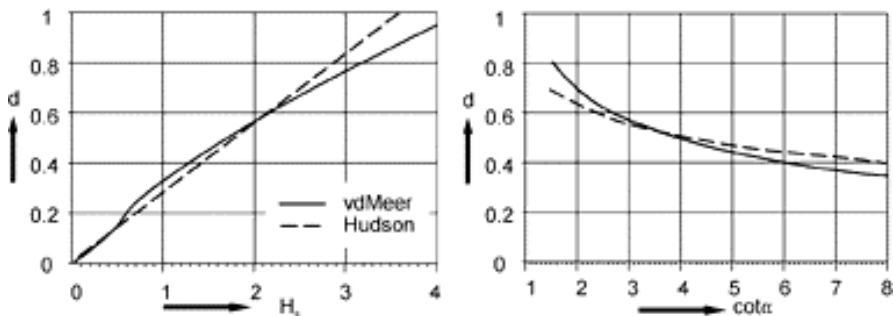


Figure 8-11 Stone diameter as a function of wave height and slope angle

Damage development

Another advantage of the Van der Meer formulae, is the possibility to take the damage development into account. This can be important for repair and maintenance policies, but also for the construction of a protection. S can be computed explicitly by rewriting equation (8.8). Figure 8-12 shows the damage as a function of wave height for stones with $d_{n50} = 0.25$ m, $\cot \alpha = 2$ and $P = 0.6$. This could be the core of a breakwater, which is exposed to waves during construction. By building the breakwater in the "moderate" season, the waves are usually lower than the design waves for the breakwater. Figure 8-12a shows the influence of the wave period on the damage, for a duration of 1000 waves and Figure 8-12b shows the influence of the number of waves with a period of 6 s. Note that a period of 6 s gives more damage than a period of 3 or 9 s, which again has to do with the transition between plunging and surging breakers. The number of waves is not so important. With these

figures and wave or wind statistics from the area, an expectation of the damage can be determined.

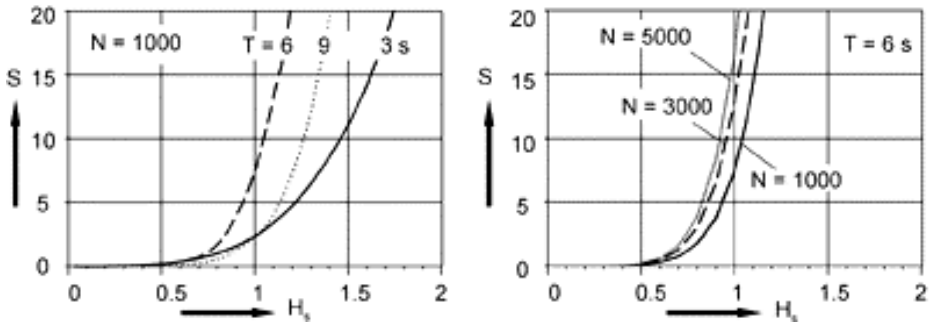


Figure 8-12 Damage as a function of wave height, wave period and storm duration

Example 8-2

A dike has to be protected with rock. The slope is 1:3 and H_s for the design waves = 1.9 m with a wave steepness, based on the average wave period, $s_m = 0.04$. What stone class is needed?

*Starting point is the Van der Meer equations. For a dike revetment, in equation 8.7, $P = 0.1$. We consider 7000 waves ($N = 7000$) and $S = 2$ (only a little damage). The surf similarity parameter, $\xi = 0.33/0.2 = 1.7$. The transition between the plunging and surging (equation 8.8), $\xi_{trans} = (6.2 * 0.1^{0.31} * \sqrt{0.33})^{1/(0.1+0.5)} = 2.5$. Hence, the plunging part of the equations has to be used. This leads to: $H_s/\Delta d_{n50} = 6.2 * 0.1^{0.18} * (2\sqrt{7000})^{0.2} * \xi^{-0.5} = 1.5$. With a value for $\Delta = 1.6$ this leads to $d_{n50} = 0.8$ m or stone class 1000-3000 kg.*

*Using Hudson's equation we would have found: $H_s/\Delta d_{n50} = (3.5 * 3)^{0.33} = 2.2$ and a $d_{n50} = 0.55$ or stone class 300-1000 kg which would be an underestimation of the necessary rock.*

Mild slopes

The relations by Hudson and Van der Meer were based on experiments with slopes in the range $\sim 1:1.5$ to $1:6$. Very mild slopes ($\cot\alpha > \sim 10$) with rock protection do exist, e.g. when a pipeline outfall on a beach is protected. In that case the breaking type is no longer plunging but spilling. Schiereck et al., 1996, did some research for this case and found that the results are even more favourable than the Van der Meer equations indicate, see Figure 8-13. In a spilling breaker the wave energy absorption is distributed quite evenly along the slope, see chapter 7, indeed resulting in a higher stability number. So, as a first approximation, the Van der Meer equations can be used even for spilling breakers (with the wave height in deep water as input value).

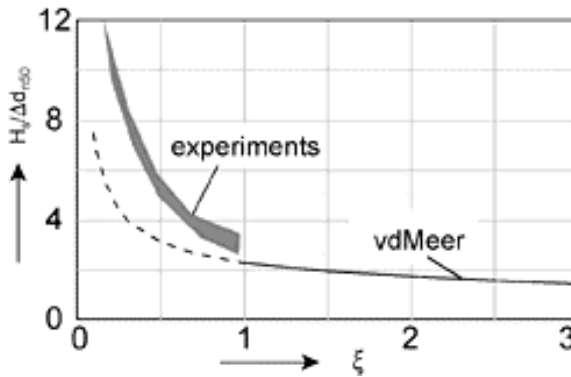


Figure 8-13 Comparison Van der Meer with mild slope experiments

8.3.3 Low crests

The Van der Meer and Hudson formulae were derived for non overtopped slopes. When slopes are overtopped, there is a certain wave transmission, see chapter 7. That means that not all energy will be destroyed on the slope and thus the stability of the armour stones will increase. For crests *above* the still water level Van der Meer (see Pilarczyk, 1990) found a reduction factor for the d_{n50} as derived from equation (8.8):

$$\text{Reduction } d_{n50} = \frac{1}{1.25 - 4.8 \frac{R_c}{H_s} \sqrt{\frac{s_{0p}}{2\pi}}} \quad (8.10)$$

where R_c is the crest height with respect to SWL, see Figure 8-14a and s_{0p} is the (deep water) wave steepness related to the peak period (T_p); the minimum value of the reduction factor is 0.8 and the maximum is 1. As a result of the wave transmission, however, armouring needs to be heavier on the other side of the breakwater and the question is whether the total damage will reduce, see also Burger, 1995. One approach for low dams is to apply the same armour units on both sides.

For crests *below* the still water level van der Meer formulated a relation for the stability (see Pilarczyk, 1990) which can be rewritten as follows:

$$\frac{H_s}{\Delta d_{n50}} = -7 \ln \left(\frac{1}{2.1 + 0.1S} \frac{h_c}{h} \right) \sqrt[3]{s_p} \quad (8.11)$$

Figure 8-14b shows some results. s_p in equation (8.11) is the *local* wave steepness instead of the deep water steepness. These formulae have been established separately and should be used with caution. Further research is needed in order to establish an overall relation for the stability increase of low crested dams.

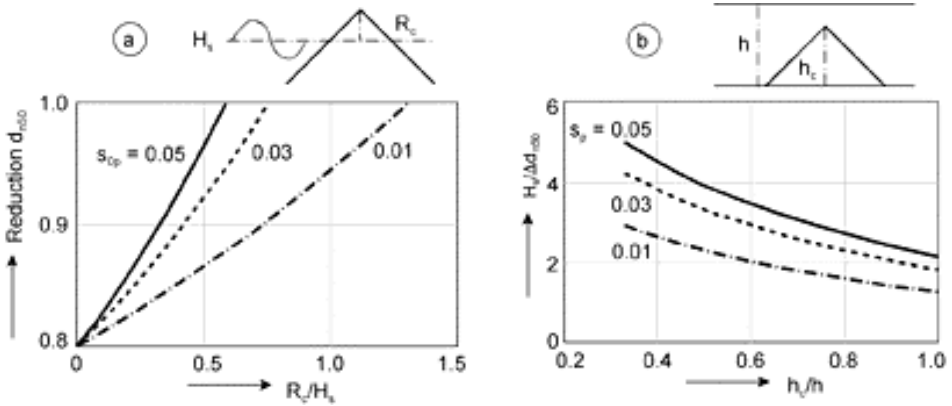


Figure 8-14 Stone stability for low crested dams

8.3.4 Toes

The toe's main function is to support the armour layer of a slope. The stones in a toe can often be smaller than those in the armour layer, since they are less heavily attacked by the waves. The waves do not break at all on deep lying toes.

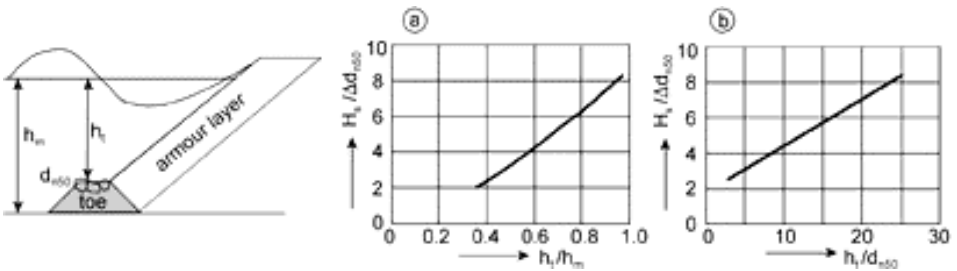


Figure 8-15 Stability of stones in toe structure

Figure 8-15a gives the results of experiments on toe stability, see CUR/CIRIA, 1991. The line in the figure represents the relation between the stability parameter and the relative toe depth:

$$\frac{H_s}{\Delta d_{n50}} = 8.7 \left(\frac{h_t}{h_m} \right)^{1.4} \tag{8.12}$$

This equation shows an increase in stability for relatively deep lying toes. The validity of this equation is restricted to situations with little damage ($S \approx 2$) and relatively deep toes ($h/h_m > 0.4$).

Figure 8-15b shows the results of research by Gerding (see d'Angremond et al., 1996). These experiments can be described with:

$$\frac{H_s}{\Delta d_{n50}} = 1.1 \left(0.24 \frac{h_t}{d_{n50}} + 1.6 \right) \quad (8.13)$$

In this expression, iteration is necessary, as d_{n50} appears at both sides of the equation. The stone size in the armour layer can be seen as the maximum stone size in a toe structure, whatever the results derived from these equations.

All of these experiments were done for breakwaters with relatively steep slopes. Toes of vertical walls lie in the antinode of a standing wave where, theoretically, only the pressure fluctuates. Wider toes may extend to the node where the velocities are at their maximum. For non-breaking waves, it is recommended to follow the procedure with the modified Shields-diagram of section 8.3.1, see also d'Angremond et al., 1996.

8.3.5 Heads

The head of a breakwater or coastal groyne is usually the most exposed part of such a structure. No systematic test results are available. The Shore Protection Manual (SPM, 1984) recommends constructing a head with stones which are twice as heavy as in the trunk or, alternatively, a head with a slope which is twice as gentle as the trunk's slope.

8.4 Stability of coherent material

8.4.1 Placed-block revetments

In revetments, particularly sea defences, placed elements, mostly made of concrete are very important. In the last twenty years, much research has been done in The Netherlands regarding the stability of placed blocks on a slope under wave attack. Therefore, this construction type will be discussed in more detail.

Placed blocks can have many shapes. Their coherence varies, blocks may be: pinched, connected with cables or geotextile, or interlocked. Another variation in the shape can be the upper side of the blocks which can be designed to reduce the wave run-up, but for this chapter this variation is not very important. Figure 8-16a gives some examples. The transition between the blocks and the underlying soil is another variable. Figure 8-16b shows some possibilities (many other combinations are possible). When the blocks are not exactly equal in height, a layer to embed the blocks is necessary to correct the height differences. This is the case when natural material like basalt is used. The extra layer is sometimes combined with a filter. Sometimes the blocks are placed directly on clay; this requires a high construction quality standard, as irregularities of the surface decrease the strength of the revetment.

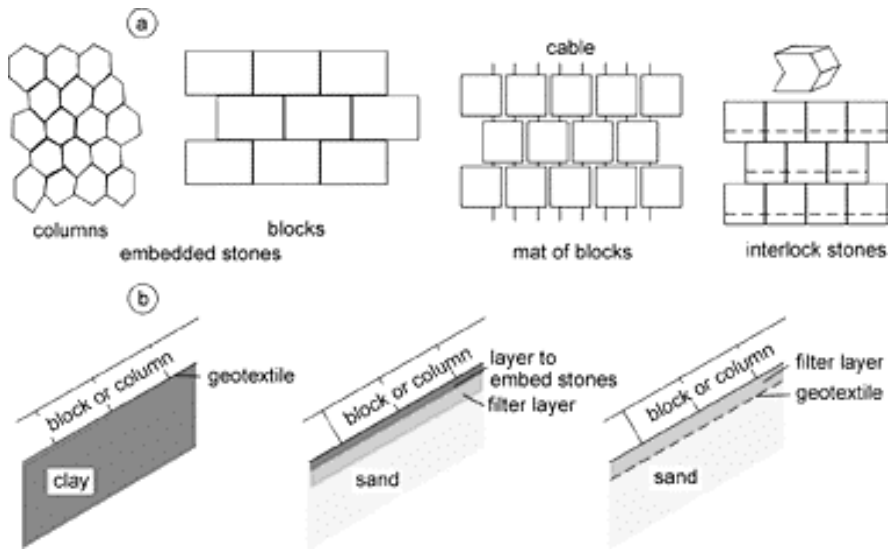


Figure 8-16 Block types and filters in revetments

Stability mechanism

In section 8.2 we saw that the characteristic length of the loading phenomenon was of the same order of magnitude as the leakage length: $L \approx \Lambda$. For loose grains and asphalt the orders of magnitude are completely different and the relation between external and internal pressures becomes very simple. When $L \approx \Lambda$, the situation is more complex and much energy has been put into fathoming the secrets of placed block stability. Figure 8-17 shows the phenomena that might play a role in the stability of placed blocks during a wave cycle. From tests and calculations it was reasoned that phenomena b and c are dominant in the process. In fact, the wave action on and under the blocks can not be separated and porous flow phenomena have to be taken into account.

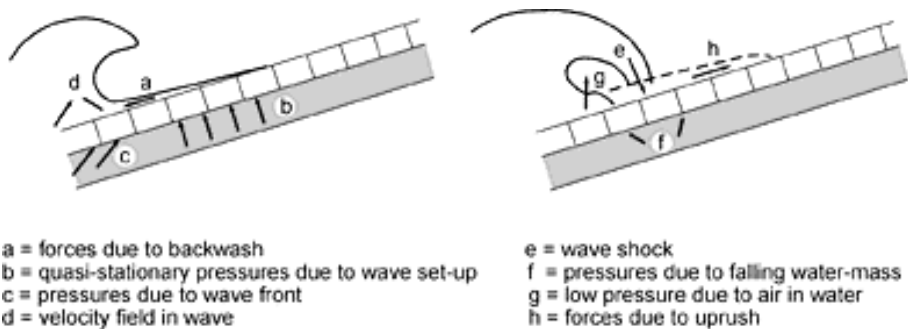


Figure 8-17 Possible loading mechanisms in block revetment

Figure 8-18a shows which forces determine the situation at maximum downrush: the pressure on the blocks is low in front of the wave, while under the blocks it is high, due to the water pressure in the filter layer caused by the propagating wave and due to the relatively high phreatic level in the slope. This causes uplift forces on the blocks.

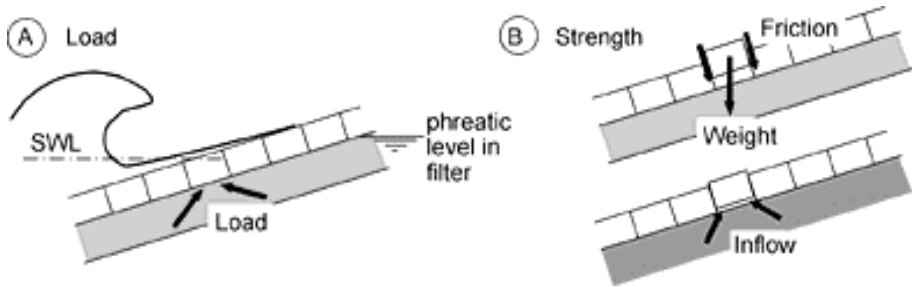


Figure 8-18 Load and strength of block revetments

Whether a block is pushed out or not depends on the strength of the revetment, in which two factors play an important role: in the first place, of course, the coherence of the blocks, which, in the case of placed blocks, is the friction between them and, even more importantly, the clamp phenomenon which will be discussed later on. The second factor is the flow towards a stone when it is pushed out. With a relatively small permeability of the filter layer, the block is sucked onto the slope because only very little water can flow into the growing hole leading to a sudden decrease of the pressure under the block, see Figure 8-18b. Both load and strength will be discussed in more detail.

Load

For the magnitude of the uplift force, the relation between the permeability of the top layer and that of the filter layer, expressed in the leakage length, Λ , is very important, see also section 8.2. To demonstrate the relative importance of permeabilities, the porous flow in the revetment is again simplified: the flow through the filter layer is assumed to be parallel to the slope while the flow through the top layer is supposed to be perpendicular to it (x is the coordinate along the slope), see Figure 8-19.

The flow in the filter layer can be expressed as:

$$v_F = -k_F \frac{d\phi_F}{dx} \quad (8.14)$$

and through the top layer:

$$v_T = k_T \frac{(\phi_F - \phi_T)}{d_T} \tag{8.15}$$

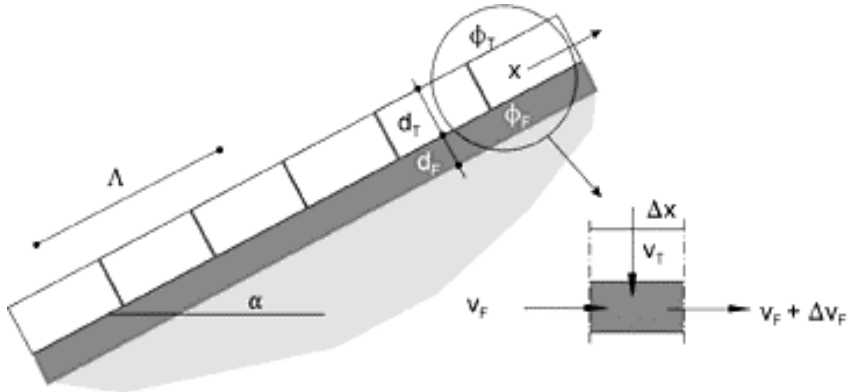


Figure 8-19 Flow through block revetment and leakage length

Based on continuity, $\Delta v_F \cdot d_F = v_T \cdot \Delta x$, see Figure 8-19, hence $v_T \approx d_F \cdot dv_F / dx$, from which follows:

$$\frac{d^2 \phi_F}{dx^2} = \frac{-k_T(\phi_F - \phi_T)}{k_F d_T d_F} = -\frac{(\phi_F - \phi_T)}{\Lambda^2} \rightarrow \phi_F - \phi_T = -\Lambda^2 \frac{d^2 \phi_F}{dx^2} \tag{8.16}$$

in which ϕ_T and ϕ_F are the piezometric head ($\phi = p / \rho g + z$) on the top layer and in the filter layer, k_T and k_F are the permeability of the top layer and filter layer and d_T and d_F are the thickness of the top layer and filter layer, respectively. From this equation it can be seen that the head difference over the top layer depends directly on Λ , defined in equation (8.3). A relatively thick and permeable filter layer and/or a relatively thick and impermeable top layer give a large Λ and hence, a large head difference over the top layer.

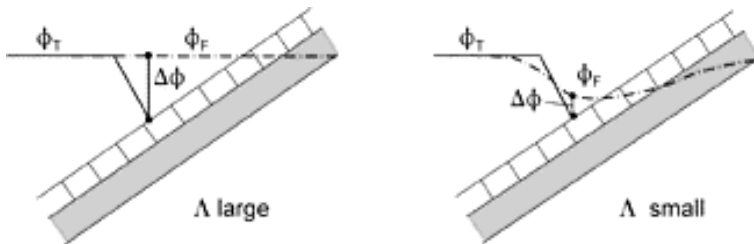


Figure 8-20 Head difference over block for large and small leakage length

This equation can be solved analytically if boundary conditions are highly schematized and if flow in the filter layer is assumed to be laminar (or more

precisely: the relation between velocity and pressure is presumed to be linear). Its description is beyond the scope of this book; the reader is referred to CUR/TAW, 1992 or to Bezuyen et al., 1990. Figure 8-20 shows the situation with a very high value of Λ and with a very small value. So, a large Λ , the leakage length, is unfavourable for the stability of the blocks and it is clear that a permeable top layer and an "impermeable" filter layer lead to the most stable structure. This means that filter layers should be kept as thin as possible!

Strength

The first element of the resistance against uplift is, of course, weight. Friction between the blocks is next and Figure 8-21a shows another potentially important mechanism in a placed block revetment, see also Suiker, 1995. When a block is lifted by the pressure from below, it will lift other blocks as well, due to friction. As a result of their geometry, this will lead to large normal forces in the blocks, which are passed on to other blocks and finally to some bordering structure.

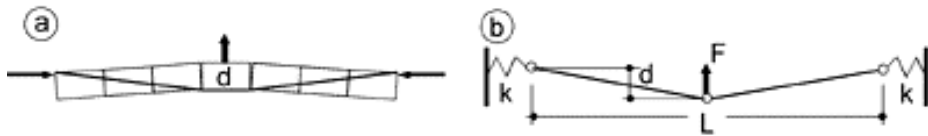


Figure 8-21 Clamping mechanism

The mechanism also works when two beams are hinged to a spring support, between two walls at a distance which is slightly smaller than the total beam length, see Figure 8-21b. From structural mechanics it is known that the maximum force, F , will be:

$$F_{\max} = \frac{16}{9} \sqrt{3} \frac{k d^3}{L^2} \quad (8.17)$$

This force is mobilized when a block is raised and there is little or no room between two blocks. The clamping will be less when slots between the blocks are present. The blocks will be placed as close to each other as possible, but slots will always be present. Taking slots into account in equation (8.17) it is found that the strength of a block revetment can be several times higher than the proper weight of the blocks, but the resulting strength depends on the slot width and the assumed value of k , as they are both uncertain.

Stability

A simple approach to determine the stability of placed blocks is as follows, see also Gerressen, 1997. The head difference across the blocks is caused by the run-down of

the waves, see chapter 7. Figure 8-22 gives the pressures along the slope.

The most unfavourable block is situated just ahead of the wave front. When the expression for the run-down from chapter 7 is used and when the only strength comes from the proper block weight, the stability is given by:

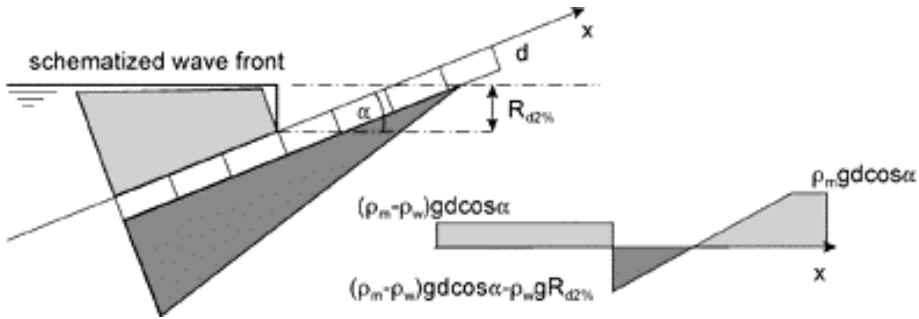


Figure 8-22 Stability of block revetment

$$(\rho_m - \rho_w)gd \cos \alpha - \rho_w g 0.33 \xi H_s = 0 \rightarrow \frac{H_s}{\Delta d} = 3 \frac{\cos \alpha}{\xi} \tag{8.18}$$

Of course, the constant 3 in equation (8.18) is only a first guess. Λ will influence the load (see Figure 8-20) and friction and clamping will influence the strength.

Results

It is obvious that, with so many assumptions and so many factors, it is impossible to give more than proportionalities in the relation between all of the involved parameters. It was found:

$$\frac{H_s}{\Delta d} \propto \left(\frac{d}{\Lambda \xi_p} \right)^{0.67} \tag{8.19}$$

For various structure types, experiments were carried out to establish the constants of proportionality, leading to the graphs presented in Figure 8-23a, which serve as an indication of the stability. There is also an "analytical" method which takes more detail into account. For more information the reader is referred to CUR/TAW, 1992.

A closer look at equation (8.19) and Figure 8-23, reveals:

- The simple stability computation using equation (8.18) is too pessimistic, but the trend is similar to equation (8.19)'s trend,
- a large Λ , leads to a low $H_s/\Delta d$, which is in line with equation (8.16) where a large Λ gives a large head-difference ($\phi_F - \phi_T$) and, hence, lower stability,

- the same holds for ξ , which is the same trend as found for loose rock, see equation (8.8)a and Figure 8-23b,
- d plays a complicated role in this equation. It is part of A , indicating that a thick top layer gives a large head-difference (equation(8.16)), which is unfavourable. But a thick top layer also means more weight and hence more strength. Assuming all other parameters in equation (8.19) are constants, it appears that: $H \propto d^{4/3}$, so a thick top layer is over-all favourable for stability.

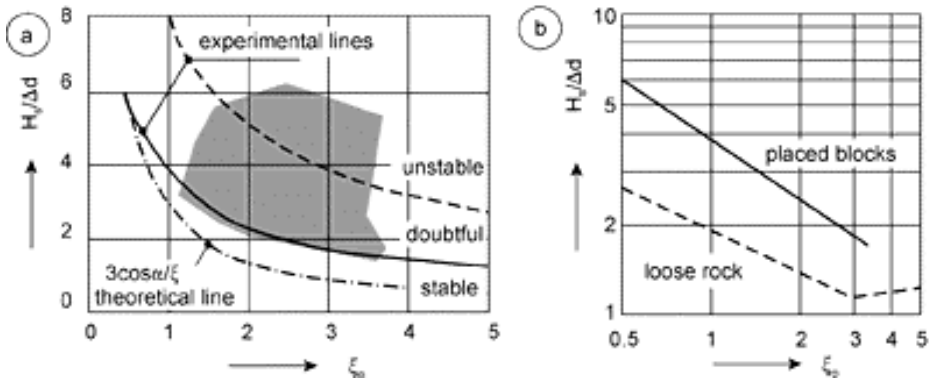


Figure 8-23 Test results for placed blocks on filter layer and comparison with loose rock

In this book no discrimination is made between the combinations of different kinds of blocks (pitched, interlocked etc.) and transitions (filter layers, geotextiles, directly on clay etc.). Compared with rip-rap, placed blocks look superior and even better results than the line presented in Figure 8-23 are possible. However, much depends on the quality control during construction and thereafter. A permeable top layer is favourable, but it can become impermeable, as a result of dirt, vegetation, shells etc. We have also seen that a thin and "impermeable" filter layer, creates a more stable situation. That is why the idea of blocks placed directly on clay is a very attractive one from a theoretical point of view. However, everything again depends on the quality of the construction, which is difficult to assure. Biological activities in the clay after construction may also have an unfavourable effect on the stability.

Example 8-3

The same dike as in Example 8-2 has to be protected with concrete blocks. The slope is 1:3 and H_s for the design waves = 1.9 m with a wave steepness, based on the average wave period, $s_m = 0.04$. When the density of the concrete is 2600 kg/m³, what is the necessary thickness?

The stability relation for block revetments in Figure 8-23 is given for ξ_p and not for ξ_m . With a peak period that is about 20 % higher than the average period ξ_p will be about 1.9. $H_s/\Delta d$ from Figure 8-23 then becomes ≈ 2.4 . In sea water, Δ becomes ≈ 1.5 , which leads to blocks with a thickness of about 0.5 m.

8.4.2 Impervious layers

Uplift

Impervious layers can be made of asphalt or concrete. The differences with blocks are that the protection forms a whole instead of consisting of separate elements and that the fluctuating wave pressures can penetrate only a limited distance from the edge of the protection. Usually there is no filter layer (the protection itself is sandtight).

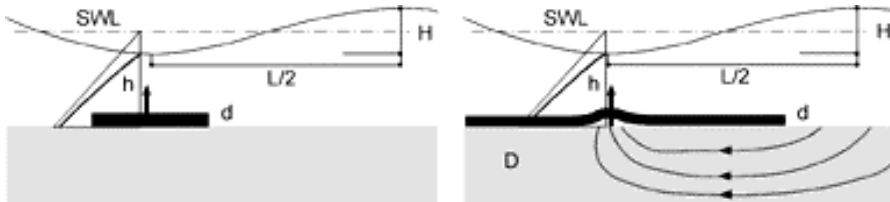


Figure 8-24 Impervious layers in waves

In the case of a protection which is shorter than a wave length, the equilibrium is simply given by:

$$(\rho_m - \rho_w)gd > \rho_w g \frac{H}{2} \frac{1}{\cosh\left(\frac{2\pi h}{L}\right)} \quad (8.20)$$

In certain places, the wave pressure on top of long protections is half the waveheight below the subsoil pressure, see Figure 8-24b. In those places, the pore pressure tries to lift the protection. This can only be effectuated if water flows into the hole between bottom and protection. TAW, 1984, has shown that this is hardly possible and that this is not an important stability factor for impervious revetments. Threats are wave impacts and porous flow due to waterlevel differences over the protection, see chapter 5.

Wave impacts

In chapter 7 the special character of wave shocks compared with the cyclic quasi-static pressures was discussed. These shocks induce stresses in the material which should not exceed the failure stress, see Figure 8-25.

The response of the layer depends, among other things, on the stiffness of the layer and the subsoil. The protection layer (asphalt or concrete) has an elasticity E (Pa) and the subsoil has a stiffness c (Pa/m). The wave impact causes a stress, σ , in the layer. Figure 8-25 shows the influence of the stiffness ratio, E/c , based on some assumed values of wave impact and layer properties. A stiff layer on a soft subsoil gives the

highest stresses. So, a concrete layer on soft clay is not a logical choice when wave impacts are to be expected.

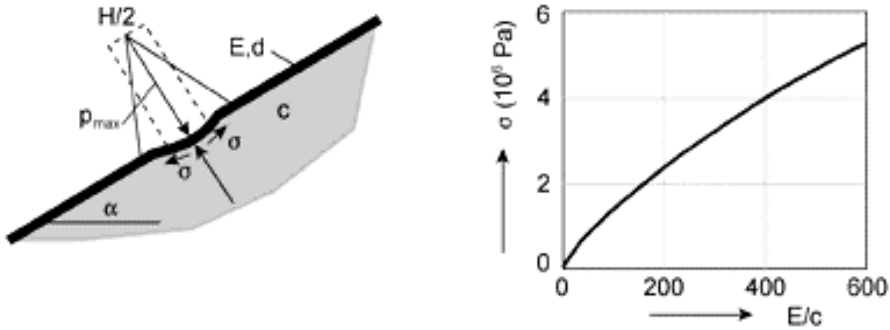


Figure 8-25 Wave impact on slope and influence material properties

To calculate the stresses, the load and response mechanism is schematized as a cushioned-spring system, see TAW, 2000. The results are:

$$\sigma = \frac{3p_{\max}}{\beta^3 H d^2} \left[1 - \exp\left(-\frac{\beta H}{2}\right) \left(\cos \frac{\beta H}{2} + \sin \frac{\beta H}{2} \right) \right] \quad \text{with } \beta = \sqrt[4]{\frac{2.65c}{E d^3}} \quad (8.21)$$

in which p_{\max} is the value for the wave pressure as mentioned in section 7.4.3 and H is the individual wave height. Typical values for the parameters involved can be found in annex A, Materials. Fatigue plays an important role in the critical stress, σ_c . Compared with a onetime load, σ_c can be 2 to 10 times lower. d has to be determined iteratively from equation (8.21), which is something that has to be done with a computer. In Figure 8-26 the results are given for asphalt concrete ($E = 10 \cdot 10^9$ Pa) on rather well compacted sand ($c = 100 \cdot 10^6$ Pa/m) and on clay ($c = 30 \cdot 10^6$ Pa/m) and a storm duration of 10-20 hours with wave impacts.

This picture shows that for mild sand slopes (< 1:3), the thickness of an asphalt concrete protection is relatively thin: < 0.2 m, even for very high waves. In that case the quasi-stationary pressures due to a high phreatic level inside determine the thickness of the layer, see chapter 5. On clay, however, wave impacts can make thick layers necessary.

Filters

A filter under an impervious protection layer is not necessary for sandtightness. For the stability of the layer as a whole it is even undesirable. The leakage length, Λ , is already infinitely high if the top layer is impervious and a filter layer does not improve the situation. When the weight of the layer is less than the excessive wave pressure, the strength of the layer must take care of the equilibrium. The situation is similar to the one in Figure 8-24b and what was said there, is also valid here. A filter

can be applied for drainage, to prevent excessive pressures against the layer due to a high phreatic level inside the slope, see Figure 8-27b and c. The effect of a filter on pressures has to be determined with a porous flow model, see chapter 5.

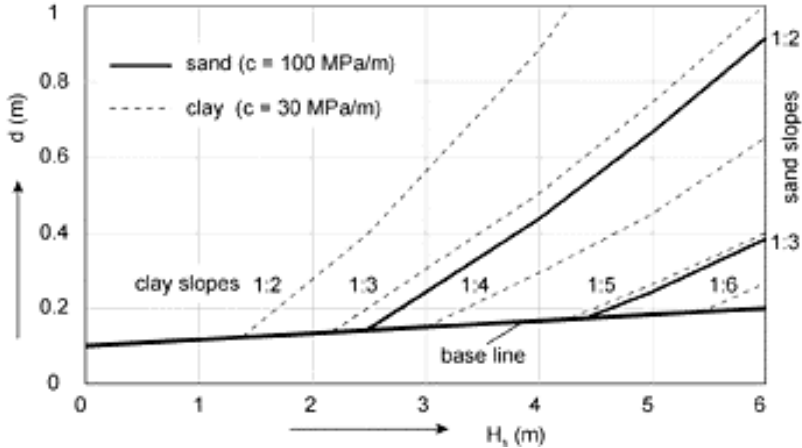


Figure 8-26 Necessary thickness of asphalt concrete on sand or clay



Figure 8-27 Influence filter under impervious layer on phreatic level

8.5 Summary

Firstly some simple relations for erosion of unprotected slopes and of bottoms in front of walls have been presented.

In this chapter the main item is stability in waves. It appears that most relations for flow situations can also be used for non-breaking waves, as long as the increased shear stress under waves is taken into account. In breaking waves, only empirical relations, like the one by Hudson:

$$M = \frac{\rho_s H_{sc}^3}{K_D \Delta^3 \cot \alpha} \quad (\text{or: } \frac{H_{sc}}{\Delta d} = \sqrt[3]{K_D \cot \alpha})$$

or Van der Meer:

$$\frac{H_{sc}}{\Delta d} = 6.2 P^{0.18} \left(\frac{S_d}{\sqrt{N}} \right)^{0.2} \xi^{-0.5} \quad (\text{plunging breakers})$$

$$\frac{H_{sc}}{\Delta d} = 1.0 P^{-0.13} \left(\frac{S_d}{\sqrt{N}} \right)^{0.2} \xi^P \sqrt{\cot \alpha} \quad (\text{surging breakers})$$

can be used.

The latter is to be preferred, since more parameters are included. The permeability of a slope is one of the most important differences between the two formulae. With Van der Meer's formulae it is also possible to calculate the damage as a function of wave parameters. **Note:** The subscript *c* indicates 'critical' values in the stability parameter $H_{sc} / \Delta d_{n50}$, thus distinguishing between stability and mobility parameters, but is not used consequently.

Typical values of the stability parameter in breaking waves, $H_{sc} / \Delta d_{n50}$, lie around 2 for rather steep, continuous slopes. Higher values are valid for mild slopes. For toes, this value can also be higher, depending on the relative depth of the toe. Low crests can lead to an increase of the stability parameter, while at the head of a dam or breakwater twice the mass computed for the trunk needs to be used.

For placed-block revetments, the mechanisms are explained and an empirical stability relation is presented. It can be concluded that block revetments of good quality, can stand greater wave loads than loose rocks. Typical values of the stability parameter, $H_{sc} / \Delta d_{n50}$, are about 1.5 - 2 times the value for loose rock.

Waves will usually not be able to lift impervious-layer revetments of some size. Wave impacts can influence the thickness of the layer. A filter is not necessary, except possibly for the drainage of excessive pressures due to tides or surges.